Singlet oxygen is not the main source of electrolyte degradation in lithium-oxygen batteries

Supplementary Information

Ceren Zor[1], Kieran D. Jones[2,3], Gregory J. Rees[1,2], Sixie Yang[1], Alexander Pateman[1], Xiangwen Gao[1], Lee R. Johnson[2,3,4]*, and Peter G. Bruce[1,2,4]*

[1]Department of Materials, University of Oxford, Oxford, U.K.

[2]The Faraday Institution, Quad One, Harwell Science and Innovation Campus, Didcot, OX11 0RA, UK

[3]Nottingham Applied Materials and Interfaces Group, School of Chemistry, University of Nottingham, Nottingham, U.K.

[4]Department of Chemistry, University of Oxford, Oxford, U.K.

*peter.bruce@materials.ox.ac.uk, lee.johnson@nottingham.ac.uk

Contents

General information

Reagents and solvents. Tetraethylene glycol dimethyl ether (tetraglyme, ≥99%) and dimethyl sulfoxide (DMSO) were purchased from Sigma-Aldrich and dried over 4 Å molecular sieves for at least three days before use (H_2O <10 ppm determined by Karl Fischer titration). Lithium bis(trifluoromethanesulfonyl)imide (LiTFSI, 99.99%, Sigma-Aldrich) was dried at 85 °C under vacuum overnight (>12 h). 9,10-Dimethylanthracene (DMA, Sigma-Aldrich, 99%) was purified by recrystallisation in ethanol, melted under constant argon flow followed by recrystallisation in ethanol. The purified powder was dried at 85 °C under vacuum overnight (>12 h). 5,10,15,20-Tetraphenyl-21*H*,23*H*-porphine (TPP), 4,5,6,7-tetrachloro-2′,4′,5′,7′-tetraiodofluorescein disodium salt (rose bengal, RB) and 1,4-dicyanobenzene were purchased (Sigma-Aldrich) and used without further purification.

Nuclear magnetic resonance (NMR) spectroscopy details. The ^{1}H NMR spectroscopy details for samples presented in **Figure S2** are as follows: Deuterated benzene (C_6D_6) was used as the lock solvent in a 1:9 solvent: sample ratio. NMR experiments were performed on a Bruker AVIII 400 (υ_0 (^{1}H) = 400.17 MHz) spectrometer equipped with 5 mm z-gradient broadband multinuclear probe. The T_1 was calculated using an inversion recovery sequence, and a 10-second recycle delay (>5T_1) was used throughout.

Samples for quantitative NMR studies (**Figure S3**) were prepared using CD_3CN as the lock solvent with a 9:1 solvent: sample ratio. The 1D and 2D NMR experiments were performed on a Bruker AVIII 600 (υ_0 (^{1}H) = 600.13 MHz, with a proton-optimised TCI HCN cryoprobe spectrometer). The T_1 was determined using an inversion recovery sequence, and a 30-second recycle delay (>5T_1) was used throughout.

^{1}H and ^{19}F NMR spectra for **Figures 3, S5 - S8** were acquired on a Bruker AV(III)400 HD or a Bruker AV(III)500 HD fitted with a 5 mm BBFO and 5 mm prodigy BBO probes, respectively. Deuterated chloroform ($CDCl_3$) was used as the lock solvent.

The chemical shifts in ^{1}H spectra were referenced to the residual (partially) non-deuterated solvent according to Fulmer et al.[1] ^{19}F NMR spectra were referenced through the solvent lock (^{2}H) signal according to the IUPAC-recommended secondary referencing method following Bruker protocols.[2] Processing of all NMR data was conducted with Bruker TopSpin or Mestrelab Research Mnova software suites.

Experimental

On-line Mass-Spectrometry Analysis

On-line MS (Thermofisher Prima BT process mass spectrometer) was used to monitor the reactivity of $^1O_2$ with the selected solvents and to quantify the CO_2 evolved during the analysis of carbonate and carboxylate formed due to degradation. For monitoring the reactivity of $^1O_2$, the gas outlet of the $^3O_2$ purged samples was connected to an on-line MS, and once a stable $^3O_2$ baseline was achieved, samples were irradiated to begin $^1O_2$ production. When irreversible reactions occur with $^1O_2$, the measured $^3O_2$ concentration decreases as O_2 has been removed from flow. It is assumed all $^1O_2$ returns to the ground state before reaching the MS due to its short half-life (10-100 µs).[3,4]

To study the amount of carbonate and carboxylate groups generated on WEs, acid and Fenton's reagent treatments were used as previously described.[5] For ^{13}C samples, the electrodes were rinsed with DME and dried under vacuum. Samples were connected to the on-line MS and Ar was used as the carrier gas. Once m/z 44 (CO_2) and m/z 45 ($^{13}CO_2$) signals stabilised, phosphoric acid was added and after the baseline stabilised for the second time, Fenton's reagent was added to decompose all the carbonate and carboxylate species, accordingly.

Carbonate analysis - Acid treatment

2 M H_3PO_4 is added to the electrodes to decompose all present inorganic carbonates to CO_2 *i.e.* Li_2CO_3 to CO_2.[5]

Carboxylate analysis – Fenton's reagent treatment

Fenton's reagent[6] was used to decompose carboxylates into CO_2. The reaction for Fenton's reagent generates radicals such as $OH^{\bullet}$ and $HO_2^{\bullet}$ which can attack electron deficient carbonyl sites such as in acetate and formate, releasing CO_2. 0.5 M $FeSO_4$ in 2 M H_3PO_3 and H_2O_2 (30%) was added to the electrodes after all CO_2 evolution from carbonate analysis had ceased.

Singlet Oxygen ($^1O_2$) Generation for On-line MS Experiments

Photocatalytic generation of $^1O_2$ was achieved using RB or TPP (<10 µM) with 530 nm or 660 nm light sources, respectively. The solutions were saturated with dry $^3O_2$ by continued sparging throughout the experiments. The experiments were either conducted in an Ar-filled glovebox or a cell connected to an on-line mass spectrometer. For experiments connected to the on-line mass-spectrometer, 20% O_2:80% Ar gas (dried over activated molecular sieves in the gas line) was bubbled into the samples whilst constantly stirring. 100% O_2 (N5.0 grade) was used for the experiments carried out in a glovebox. The chemical stability of the photosensitiser with the electrolyte and its electrochemical stability at 3.8 V are important selection criteria. Hence, RB was only used for chemical experiments, while TPP which is stable at higher oxidising potentials (**Figure S1**) was used in the electrochemical experiments.

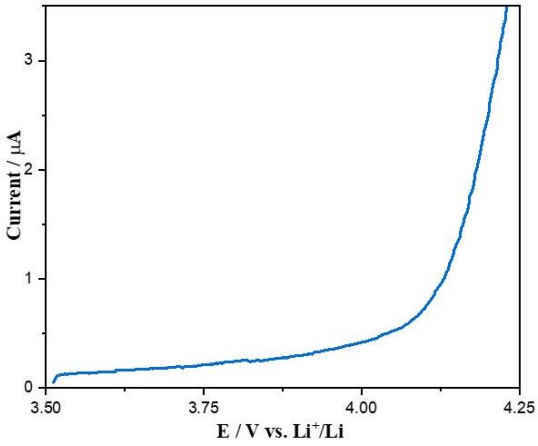

Figure S1. Cyclic voltammogram of 7 μM TPP in 0.1 M LiTFSI and tetraglyme. The CV was recorded with a planar Au working and counter electrodes and a fritted delithiated $LiFePO_4$ reference electrode at a scan rate of 100 mV s^{-1}.

$^1O_2$ oxidation of DMSO

DMSO was treated with $^1O_2$ and O_2 consumption was monitored via online-mass spectrometry using the procedures described above (**Scheme S1**). Dimethyl sulfone ($DMSO_2$) was determined to be the major product, and the spectroscopic data (**Figure S2**) is consistent with those reported previously.[7]

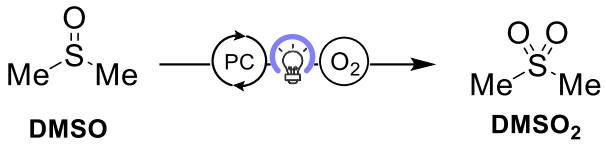

Scheme S1. Photo-oxidation of DMSO via singlet oxygen.

FTIR spectra of the resulting mixture were recorded in an N_2-filled glovebox using a Thermo Fischer Nicolet iS50 FTIR Spectrometer. The spectra showed new peaks consistent with $DMSO_2$ (**Figure S2**). **FTIR** (cm^{-1}) 1142 ($\nu_{as}SO_2$), 763 (ν_sCSC), 499 (δOSO), 465 (γ or ρSO_2).

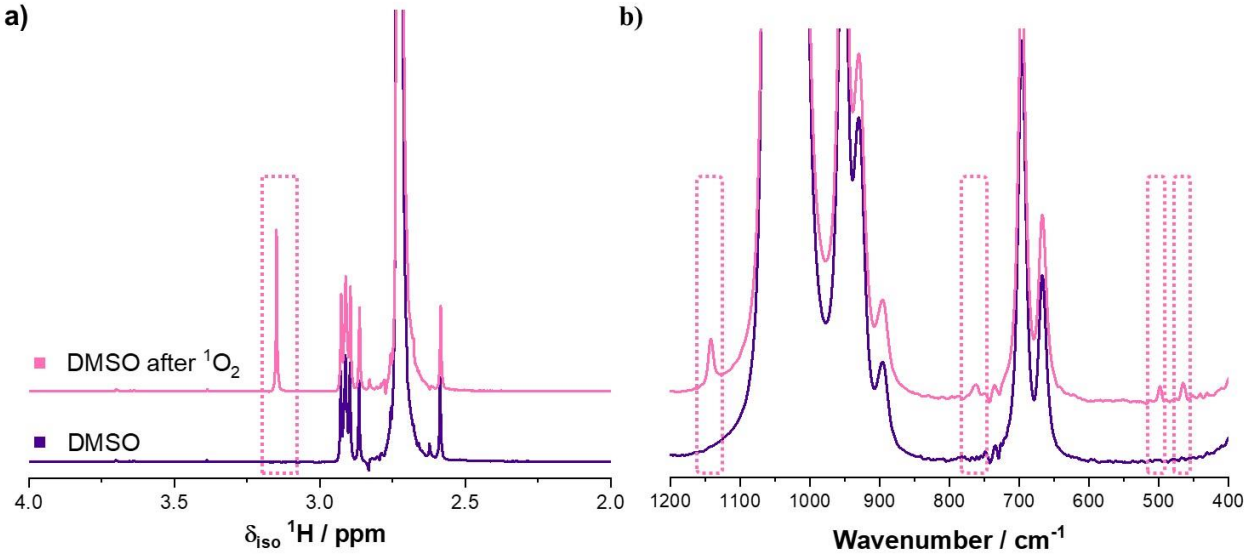

Figure S2. **a**) ^1H NMR (400 MHz, C_6D_6, 298.1 K) spectra of the DMSO reaction solution before and after exposure to $^1O_2$. **b**) FTIR spectra for DMSO (purple) and $^1O_2$ treated DMSO (pink, $DMSO_2$ peaks highlighted.

Determination of $^1O_2$ formation rate and comparison to the cell

The amount of $^1O_2$ generation was confirmed by NMR spectroscopic experiments. DMA (75 mM) and TPP (7 µM) were dissolved in 0.1 M LiTFSI tetraglyme electrolyte and 100% dry O_2 was bubbled into the solution. The light was turned on after 2 h to ensure that the solution was initially saturated with $^3O_2$ before $^1O_2$ generation. The duration of light exposure was recorded, and samples were analysed by quantitative NMR to quantify DMA and 9,10-dimethyl-9,10-dihydro-9,10-epidioxyanthracene ($DMAO_2$) (**Figure S3**). The amount of $DMAO_2$ was calculated by integration of the NMR data, and the rate of $^1O_2$ generation under these photochemical conditions was estimated to be 1.56×10^{-5} mol min^{-1} assuming 100% capture of $^1O_2$ by DMA. The efficiency of the $^1O_2$ generation was tested under an applied potential of 3.8 V and the amount of $DMAO_2$ is not affected by the voltage. Correcting for volume, 750 µL of electrolyte gives a rate per volume of 2.08×10^{-2} mol $^1O_2$ $L^{-1}min^{-1}$. The rate of $^1O_2$ formation in a cell containing 100 µL electrolyte and 1 mg carbon electrode discharging at 100 mA g^{-1}_{carbon}, and assuming 2% $^1O_2$ generation, is 6.12×10^{-6} mol $^1O_2$ $L^{-1}min^{-1}$ which is ~1000 times less than that found in in the online-MS experiments. Assuming the steady-state concentration of $^1O_2$ is directly proportional to the rate of formation, then the $^1O_2$ concentration is also ~1000 greater in our degradation analysis compared to the cell and can be considered a harsher test of stability.

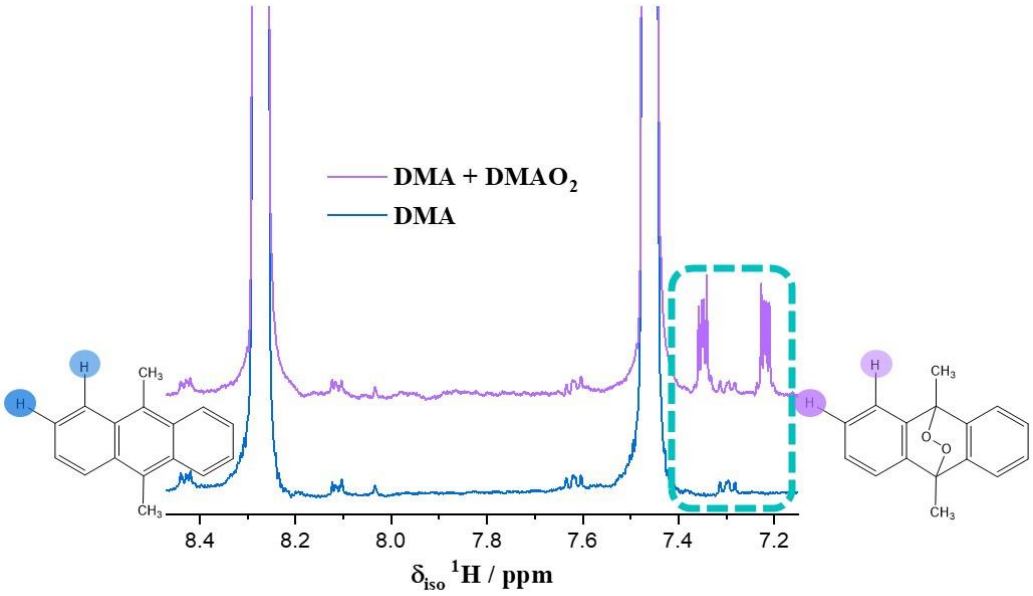

Figure S3. The ^1H NMR (600 MHz, CD_3CN, 298.1 K) spectra of a solution containing 75 mM DMA (*bottom*) and a $^1O_2$ exposed solution (*top*) show resonances for DMA and $DMAO_2$. The aromatic peaks for $DMAO_2$ are marked in the dashed box.

Electrode Preparation

For ^{13}C-PTFE composite working electrodes (WEs), amorphous carbon-13 powder (^{13}C, Sigma-Aldrich) was treated at 900 °C under Ar:H_2 (95:5, v/v) flow for 5 h. The carbon powder was transferred to an Ar-filled glovebox. The WEs were prepared in an Ar-filled glovebox by mixing ^{13}C and PTFE powder in an agate mortar. 10 mg of the composite material was pressed into a 7 mm diameter. The pellet was then pressed onto a stainless-steel mesh (100 mesh, Advent-RM) current collector.

Li_2O_2-preloaded working electrodes (^{13}C-Li_2O_2 WEs) were prepared by grinding carbon-13 powder and in-house synthesised Li_2O_2 (80:20 w/w), and adding 15% PTFE powder to this mixture. Similar to ^{13}C WE, ^{13}C- Li_2O_2 composite material was pressed into 7 mm diameter pellets with 10 mg material loading.

$LiFePO_4$ was used as the counter and reference electrode material. To make $LiFePO_4$ electrodes, $LiFePO_4$, Super P, and PTFE (in water) were mixed in an 80:10:10 w/w ratio with isopropanol into a homogenous paste. This paste was cast on stainless steel mesh. The $LiFePO_4$ electrodes were chemically delithiated to ~20 % total capacity (Li_xFePO_4, x<1). For this, the electrodes were soaked in 1.5 mL acetic acid (Aldrich), 3.6 ml 30% H_2O_2 (Aldrich) and 250 ml MilliQ water for 20 minutes.[9] The electrodes were washed with MilliQ water (18.2 MΩ cm) and isopropanol until all the acetic acid was removed, dried under vacuum at 85 °C overnight, and transferred into an Ar-filled glovebox.

Electrochemical Experiments

The effect of $^1O_2$ under applied potential was investigated by applying a constant potential of 3.8 V $Li|Li^+$ for 12 hours whilst photochemically generating $^1O_2$ in-situ. The same electrochemical experiments were repeated with $^3O_2$ (without turning on the light source). The electrodes were carbon-13 (WE), $LiFePO_4$ (CE), and delithiated $LiFePO_4$ (REF). The electrolyte was 0.1 M in LiTFSI in tetraglyme containing 7 µM TPP.

^{13}C-Li_2O_2 WEs were used to investigate the effect of Li_2O_2 on degradation and for these experiments the cell was charged under Ar atmosphere at a constant potential of 3.8 V.

Cyclic voltammetry was performed in a heart-shaped flask with a planar Au working and counter electrodes and a fritted delithiated $LiFePO_4$ reference electrode at a scan rate of 100 mV s^{-1}.

Singlet Oxygen Induced Degradation Studies (Batch)

Photochemical Set-up

Photochemical reactions were conducted using green LED bulbs (5 W). Lamps were positioned with a bulb-to-vial distance of approximately 10-15 mm and fan cooling was used to maintain an external temperature of ~25-30 °C (**Figure S4**). Internal temperatures were measured to not exceed 27 °C. All reactions were magnetically stirred at 500 rpm using a PTFE coated stirrer bar.

Warning: **Oxygenated ethers**. Extended storage of oxygenated ether solvents, particularly in the absence of a stabiliser, is hazardous due to the accumulation of organic peroxides which can lead to unexpected explosions.[10] Ensure temperatures do not exceed 30 °C due to the risk of detonation.

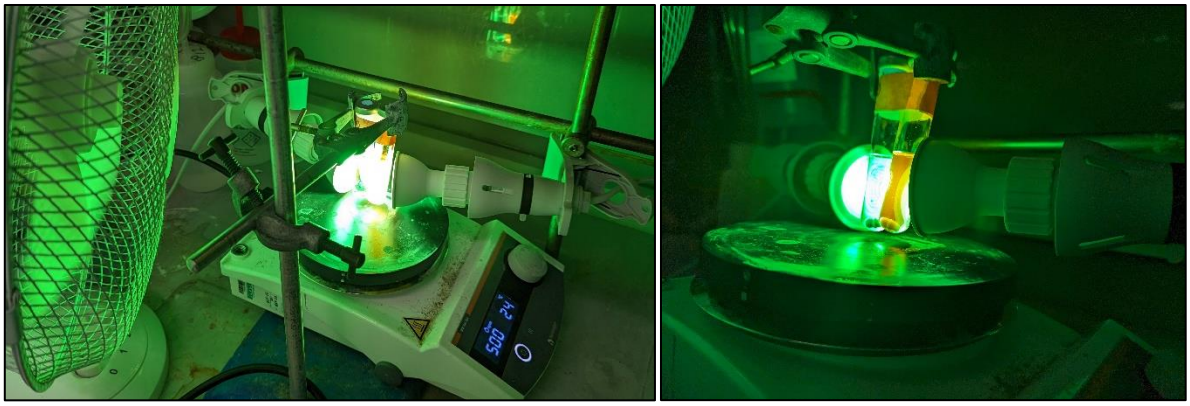

Figure S4. Photochemical set-up for reactions using green LED bulbs (5 W).

Tetraglyme & LiTFSI Experiments

Photosensitisation of triplet oxygen with RB or TPP has been reported as an efficient method for $^1O_2$ formation and subsequent $^1O_2$ mediated C-H hydroperoxidation of cyclic ethers (such as THF) and activated linear ethers.[11] Having successfully reproduced these results with THF (not shown), the method was deemed suitable for the evaluation of tetraglyme and 1 M LiTFSI in tetraglyme stability to $^1O_2$ by both flow and batch. A modified general procedure deviating from Su, M and co-authors' method is described below. Results for tetraglyme and 1 M LiTFSI in tetraglyme are summarised in **Tables S1** and **S2,** respectively. In both cases, no change to tetraglyme or the TFSI anion following prolonged exposure to $^3O_2$ with and without photocatalyst, nor when irradiated with green light in the absence of photocatalyst was detected by ^1H and ^{19}F NMR spectroscopies (**Figure S5-7**). Under reaction conditions producing $^1O_2$ (*Entry 4,* **Tables S1 & S2**) new resonances were observed in the ^1H NMR spectra at 11.0 – 8.5 ppm and 5.5 – 4.5 ppm suggesting tetraglyme degradation (**Figure S5 & S6, Scheme S2**). Conversely, the TFSI anion showed no change by ^{19}F NMR spectroscopy following prolonged exposure to $^1O_2$ (**Figure S7**), even with organic hydroperoxide species present, suggesting stability to both $^1O_2$ and tetraglyme degradation products.

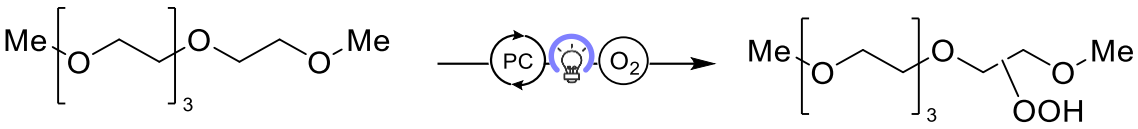

Scheme S2. Photo-oxidation of tetraglyme via singlet oxygen.

General procedure: An oven-dried microwave vial equipped with a stirrer bar was taken inside a glovebox (nitrogen atmosphere) before the addition of tetraglyme solution (with or without 1 M LiTFSI) and rose bengal stock solution (if using) to a total volume of 4 mL. The vial was sealed with a septum-lined cap, removed from the glovebox and sparged with oxygen (5-10 min) before irradiating according to the described photochemical setup for 18 h. An internal standard, 1,4-dicyanobenzene (5.1 mg, 0.04 mmol, 0.01 M), was added to the resulting solution, a 50 µL aliquot was taken, added to $CDCl_3$ (0.75 mL) and NMR spectroscopies measured.

Table S1. Stability test of tetraglyme under the photocatalytic generation of singlet oxygen.[a]

Entry	Photocatalyst	Light source	Degradation detected
1	None	None	NPD
2	None	Green	NPD
3	**RB**	None	NPD
4	**RB**	Green	Traces

[a]Reaction conducted according to the *general procedure*: Photocatalyst (1×10^{-5} M), tetragylme (4 mL), O_2, irradiated for 18 h. NPD = No products detected. Trace is denoted when the concentration of products is <1 mM.

Table S2. Stability test of 1 M LiTFSI tetraglyme solution under the photocatalytic generation of singlet oxygen.[a]

Entry	Photocatalyst	Light source	Degradation detected	
			Tetraglyme	LiTFSI
1	None	None	NPD	NPD
2	None	Green	NPD	NPD
3	**RB**	None	NPD	NPD
4	**RB**	Green	Trace	NPD

[a]Reaction conducted according to the *general procedure*: Photocatalyst (1×10^{-5} M), 1 M LiTFSI tetragylme (4 mL), O_2, irradiated for 18 h. NPD = No products detected. Trace is denoted when the concentration of products is <1 mM.

Supplementary Note 1: Tetraglyme degradation calculations

As indicated by ^{1}H NMR spectroscopy, tetraglyme underwent degradation in the presence $^1O_2$ with observable signals in the regions of 11.0 – 8.5 ppm and 5.5 – 4.5 ppm (**Figure 3 & S5, S6 & S8**). These resonances are in the expected regions for organic hydroperoxide proton (OOH) and associated tertiary proton (OCH) environments, respectively. Given tetraglyme contains multiple sites vulnerable to oxidation (eight α-CH_2 positions), a series of mono, bis, or greater hydroperoxide species are the likely contributors to the observed signals. Under the assumption that each new resonance in the region of 11.0 – 8.5 ppm corresponds to a reacted $^1O_2$, we note seven significant peaks with the concentration for each of these new species to be approximately 0.2 – 0.8 mM as determined by ^{1}H NMR spectroscopic analysis. Thus, the estimated maximum concentration of accumulated $^1O_2$ products is ca. 5.6 mM, with moles of $^1O_2$ consumed approximated to be 2.2 $\times 10^{-5}$ mol.

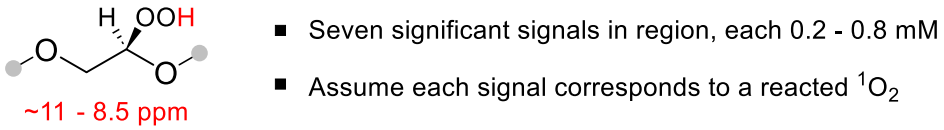

Scheme S3. Photo-oxidation sites at tetraglyme by singlet oxygen and highlighting the new ^{1}H NMR resonance region of 11.0 – 8.5 ppm

To understand the impact of tetraglyme degradation by $^1O_2$ on the cell, we can compare the amount of degradation products formed per $^1O_2$ in model experiments and relate this to known $^1O_2$ formation in the cell. The NMR spectroscopic analysis above suggests that the rate of $^1O_2$ formation is ca. 2.08 $\times 10^{-2}$ mol $^1O_2$ $L^{-1}min^{-1}$ for photochemical reactions, considering the variance between our $^1O_2$ quantification and degradation (Batch) studies, this value is expected to be a minimum rate and thus an overestimate of the impact of $^1O_2$. Assuming the photocatalyst was active for only 4 hours before bleaching, the total amount of $^1O_2$ formed is ca. 5.0 moles $^1O_2$ L^{-1}. Taking the concentration of degradation products above and normalising this to the total $^1O_2$ formed per unit volume, the moles of degradation products per mole of $^1O_2$ is 1.1 x 10^{-3} mol mol^{-1}. Assuming 2 % of all moles of oxygen form $^1O_2$ in the cell during charge, then the percentage of degradation due to singlet oxygen in the cell is ca. 2.2 x 10^{-3}%. Assuming a worst-case scenario where 10 % of oxygen used within the cell forms $^1O_2$, then the estimated amount of degradation is still only 0.01 % of the discharge product which is not consistent with the 10 % found in practical cells. In summary, $^1O_2$ degradation pathways of the solvent and salt are likely minor compared to other challenges existing in state-of-the-art systems.

Spectra

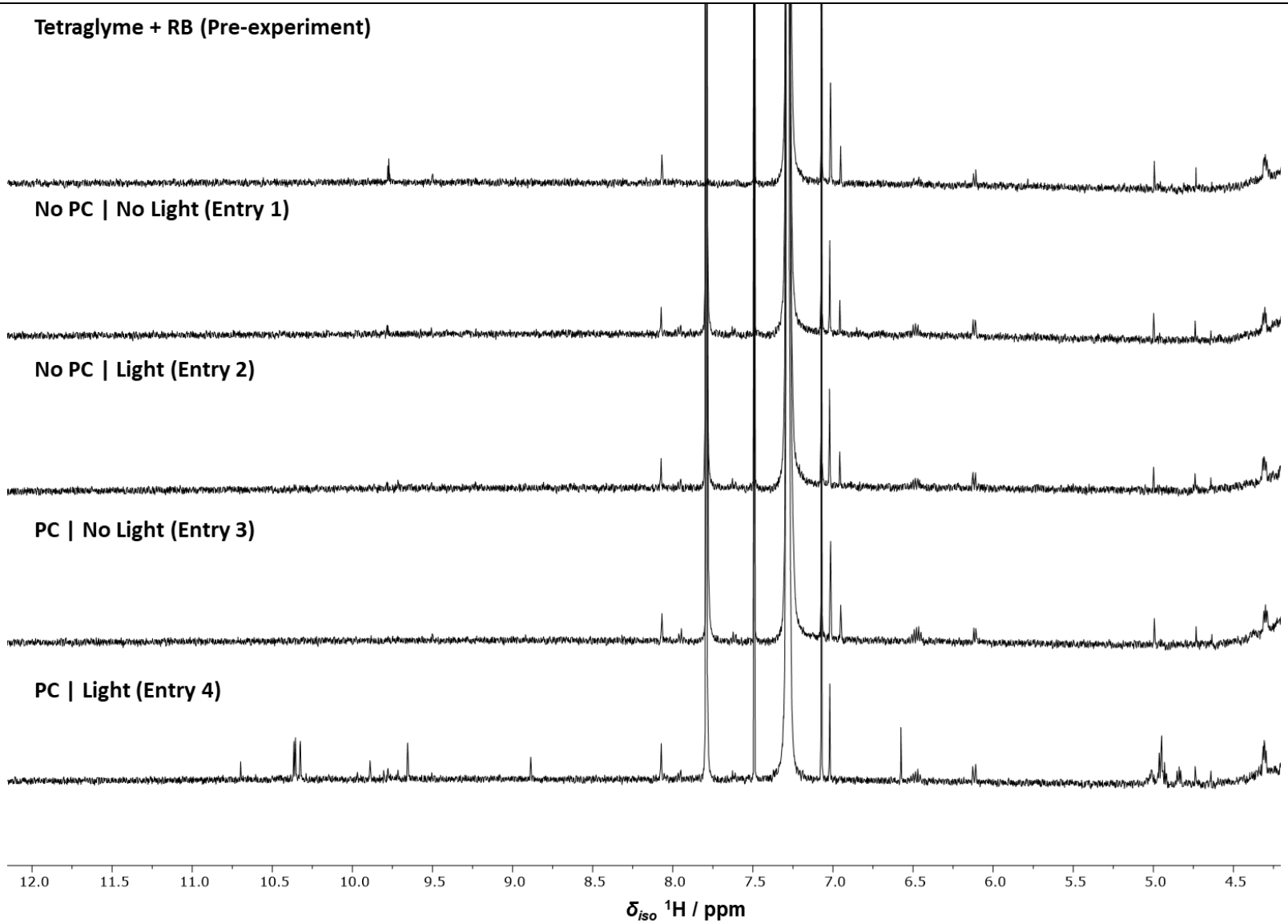

Figure S5. Highlighted baseline of ^{1}H NMR (500 MHz, $CDCl_3$, 298 K) spectra of tetraglyme experiments from **Table S1**, notable degradation products detected only under singlet oxygen forming reaction conditions (*entry 4*). PC = photocatalyst.

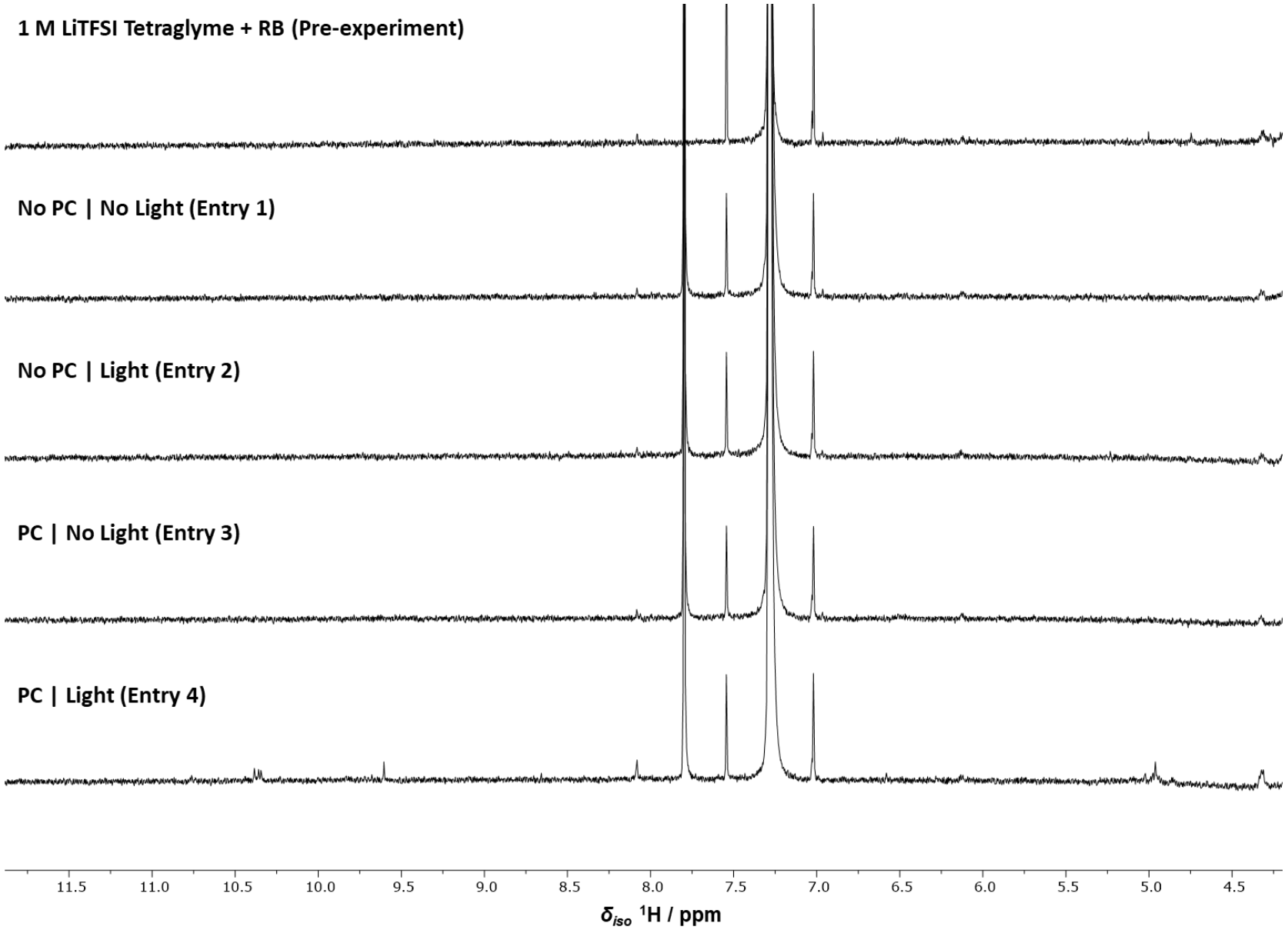

Figure S6. The highlighted baseline of ^{1}H NMR (400 MHz, $CDCl_3$, 298 K) spectra of 1 M LiTFSI tetraglyme experiments from **Table S2**, notable degradation products detected only under singlet oxygen forming reaction conditions (*entry 4*). PC = photocatalyst

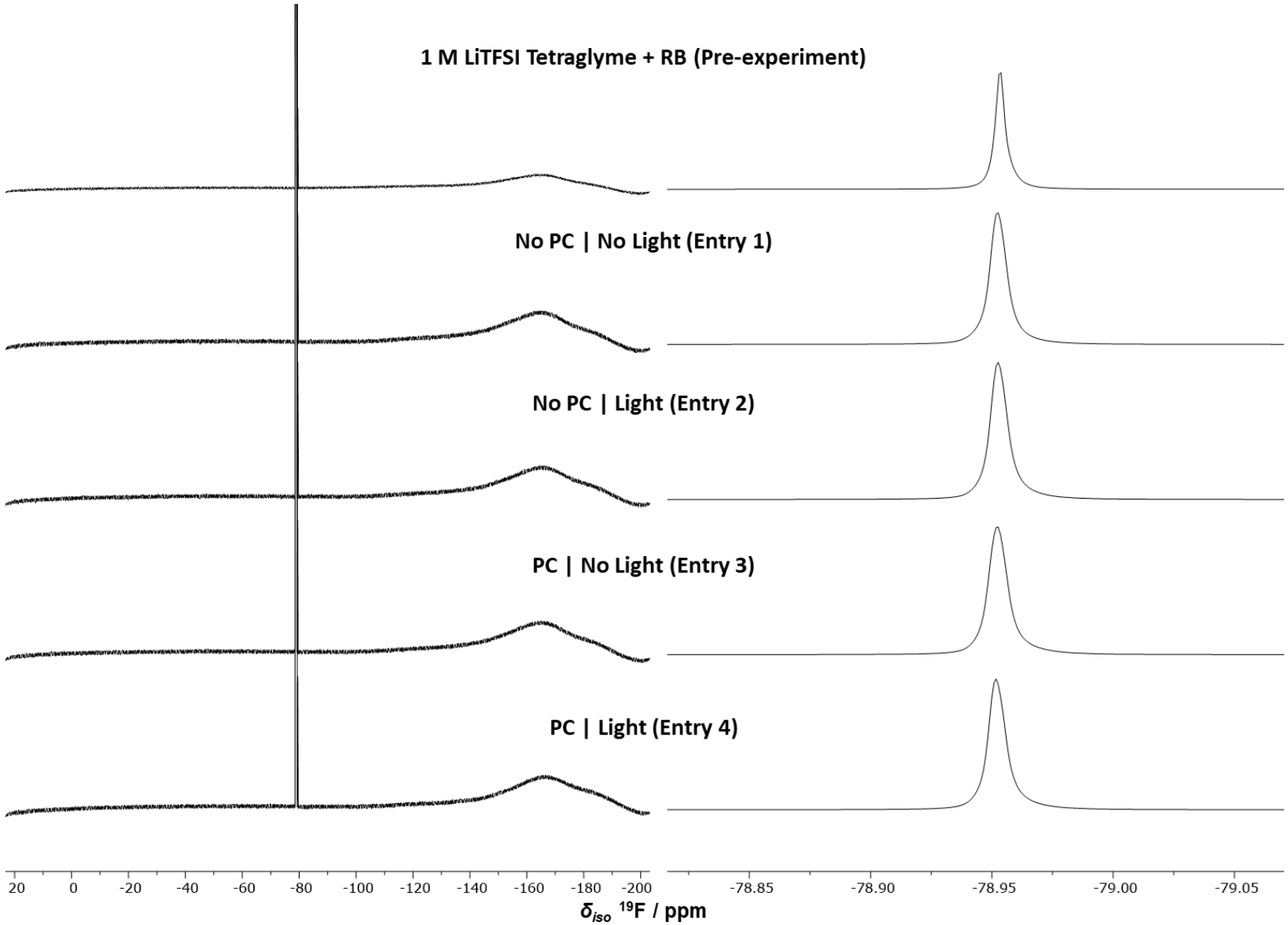

Figure S7. ^{19}F NMR (377 MHz, $CDCl_3$, 298 K) spectra of 1 M LiTFSI tetraglyme experiments from **Table S2** indicating complete stability of LiTFSI to $^1O_2$ under photochemical conditions. *Left*) Full spectra window shown, the broad resonance at ~ 170 ppm is the PTFE probe background. *Right*) Highlight of LiTFSI singlet region indicating no change in multiplicity.

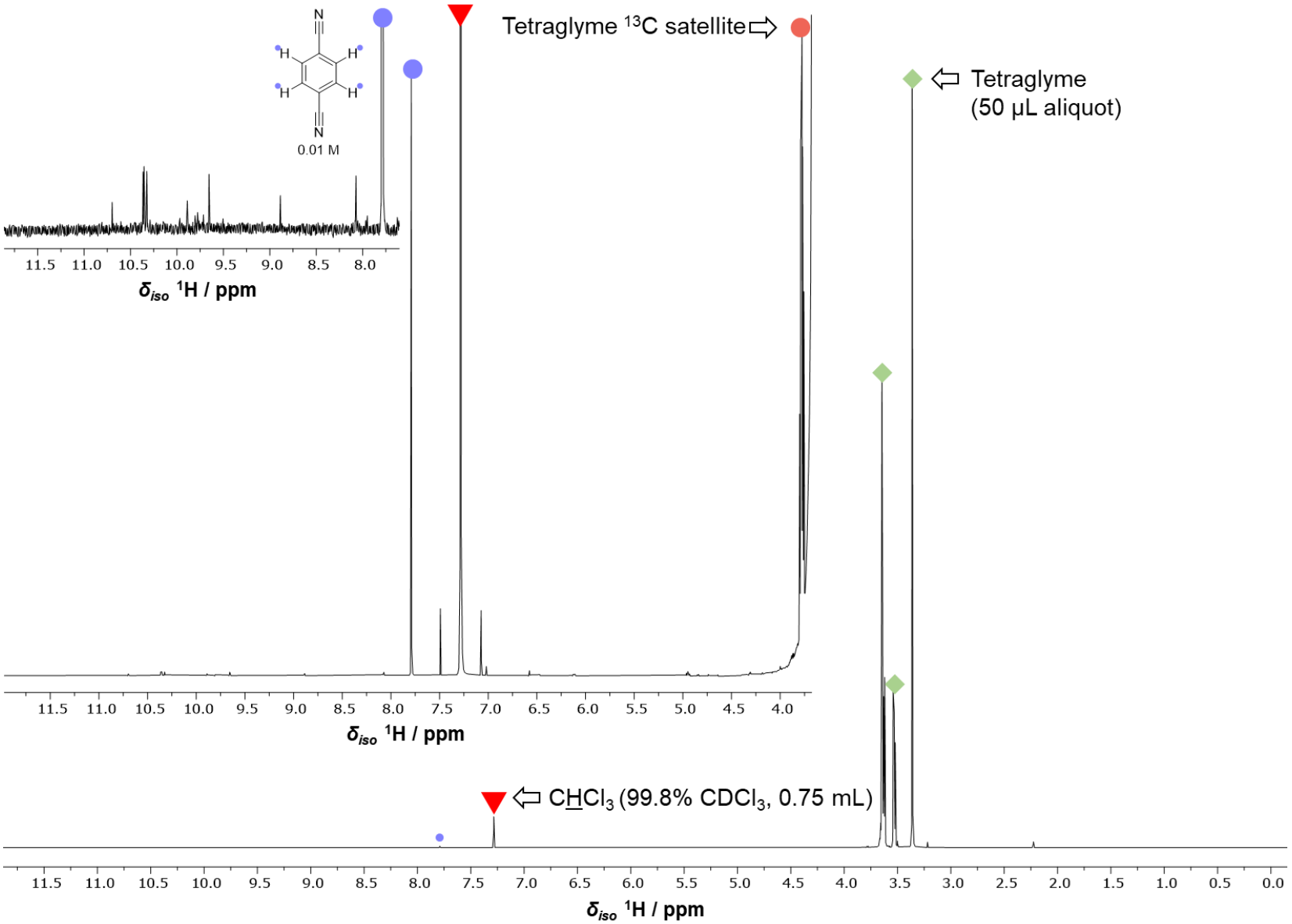

Figure S8. ^{1}H NMR (500 MHz, $CDCl_3$, 298 K) spectroscopy highlighting degraded tetraglyme attributed to singlet oxygen (**Table S1**, *entry 4*). Internal standards in the tetraglyme solution (0.01 M) and tetraglyme ^{13}C carbon satellites are shown to indicate the trace quantities of degradation products.

References

(1) Fulmer, G. R.; Miller, A. J. M.; Sherden, N. H.; Gottlieb, H. E.; Nudelman, A.; Stoltz, B. M.; Bercaw, J. E.; Goldberg, K. I. NMR Chemical Shifts of Trace Impurities: Common Laboratory Solvents, Organics, and Gases in Deuterated Solvents Relevant to the Organometallic Chemist. *Organometallics* **2010**, *29* (9), 2176–2179. https://doi.org/10.1021/om100106e.

(2) Harris, R. K.; Becker, E. D.; Menezes, S. M. C. de; Granger, P.; Hoffman, R. E.; Zilm, K. W. Further Conventions for NMR Shielding and Chemical Shifts (IUPAC Recommendations 2008). *Pure Appl. Chem.* **2008**, *80* (1), 59–84. https://doi.org/10.1351/pac200880010059.

(3) Boneva, M.; Ivanov, S. K.; Oliveros, E.; Braun, A. M. Singlet Oxygen Quenching by Tertiary Alkyl Ethers. *J. Photochem. Photobiol. Chem.* **1992**, *68* (3), 343–351. https://doi.org/10.1016/1010-6030(92)85243-N.

(4) Schweitzer, C.; Schmidt, R. Physical Mechanisms of Generation and Deactivation of Singlet Oxygen. *Chem. Rev.* **2003**, *103* (5), 1685–1758. https://doi.org/10.1021/cr010371d.

(5) Ottakam Thotiyl, M. M.; Freunberger, S. A.; Peng, Z.; Bruce, P. G. The Carbon Electrode in Nonaqueous Li–O2 Cells. *J. Am. Chem. Soc.* **2013**, *135* (1), 494–500. https://doi.org/10.1021/ja310258x.

(6) Fenton, H. J. H. LXXIII.—Oxidation of Tartaric Acid in Presence of Iron. *J. Chem. Soc. Trans.* **1894**, *65* (0), 899–910. https://doi.org/10.1039/CT8946500899.

(7) Kwabi, D. G.; Batcho, T. P.; Amanchukwu, C. V.; Ortiz-Vitoriano, N.; Hammond, P.; Thompson, C. V.; Shao-Horn, Y. Chemical Instability of Dimethyl Sulfoxide in Lithium–Air Batteries. *J. Phys. Chem. Lett.* **2014**, *5* (16), 2850–2856. https://doi.org/10.1021/jz5013824.

(8) Mourad, E.; Petit, Y. K.; Spezia, R.; Samojlov, A.; Summa, F. F.; Prehal, C.; Leypold, C.; Mahne, N.; Slugovc, C.; Fontaine, O.; Brutti, S.; Freunberger, S. A. Singlet Oxygen from Cation Driven Superoxide Disproportionation and Consequences for Aprotic Metal–O2 Batteries. *Energy Environ. Sci.* **2019**, *12* (8), 2559–2568. https://doi.org/10.1039/C9EE01453E.

(9) Lepage, D.; Michot, C.; Liang, G.; Gauthier, M.; Schougaard, S. B. A Soft Chemistry Approach to Coating of LiFePO4 with a Conducting Polymer. *Angew. Chem. Int. Ed.* **2011**, *50* (30), 6884–6887. https://doi.org/10.1002/anie.201101661.

(10) Mason, D. Those Pesky Peroxides…. *J. Chem. Health Saf.* **2014**, *21* (3), 13–15. https://doi.org/10.1016/j.jchas.2013.12.011.

(11) Sagadevan, A.; Hwang, K. C.; Su, M.-D. Singlet Oxygen-Mediated Selective C–H Bond Hydroperoxidation of Ethereal Hydrocarbons. *Nat. Commun.* **2017**, *8* (1), 1812. https://doi.org/10.1038/s41467-017-01906-5.